Easily Constructed Spectroelectrochemical Cell for Batch and Flow Injection Analyses

Paul A. Flowers* , Margaret A. Maynor and Donald E. Owens
Department of Chemistry and Physics, The University of North Carolina at Pembroke, POB 1510, Pembroke, North Carolina 28372-1510

published in Analytical Chemistry, 2002, 74(3), 720-723

The design and performance of an easily constructed spectroelectrochemical cell suitable for batch and flow injection measurements are described. The cell is fabricated from a commercially available 5 mm quartz cuvet and employs 60 ppi reticulated vitreous carbon as the working electrode, resulting in a reasonable compromise between optical sensitivity and thin layer electrochemical behavior. The spectroelectrochemical traits of the cell in both batch and flow modes were evaluated using aqueous ferricyanide and compare favorably to those reported previously for similar cells.

INTRODUCTION

Since their introduction nearly forty years ago,[1] spectroelectrochemical (SEC) techniques have been extensively applied to fundamental studies of electrode processes and related phenomena.[2, 3] These techniques have been less frequently employed for purely analytical purposes, i.e., measurement of analyte concentration, such applications being motivated primarily by the enhanced selectivity associated with control of the electrolysis potential. The most recent addition to the body of work in this area has been a series of articles by Heineman et al. describing various analytical aspects of an SEC

sensor employing a surface modified optically transparent electrode and attenuated total reflectance sampling.[4]

Analytical applications of SEC techniques are facilitated by rugged cells of adequate optical sensitivity and thin layer electrochemical behavior that permit rapid, reproducible measurements. Related to the authors' ongoing work in developing SEC assays for clinical and environmental applications, efforts have been directed toward designing such a cell that both facilitates the numerous replicate measurements associated with analytical method development and achieves the high sample throughput generally desired in method application. Proven most appropriate to these design objectives has been a cell with a reticulated vitreous carbon (RVC) working electrode that may be either syringe filled with sample (batch mode) or used as a detector in flow injection analysis. First used as an optically transparent electrode (OTE) by Norvell and Mamantov, [5] RVC has become widely recognized as a versatile working electrode material. It is readily available and inexpensive, and its porosity and thickness may be selected to yield a suitable compromise between optical and electrochemical characteristics.[6] Though numerous reports on the use of RVC electrodes in various flow electrolysis applications have been published,[7-15] only a few have entailed SEC measurements[8,9,11] and just one of these[9] involved use of the RVC as an OTE (the others employed downstream optical sampling).

Described here are the design and characteristics of an RVC-SEC cell that may be used for both flow injection and batch measurements. The cell is easily constructed without machining, glassworking or epoxies, employs paraffin wax film as gasket material, and may typically be used for hundreds of sample analyses before leakage or clogging requires its reassembly. Results of measurements using aqueous ferricyanide are presented that demonstrate the cell's favorable analytical characteristics in both batch and flow injection modes.

EXPERIMENTAL

Reagents. Reagent grade potassium nitrate and potassium ferricyanide were used as received from Fisher Scientific. Solutions were prepared using distilled water, stored under refrigeration, and typically used within three days of preparation.

Cell Construction. The cell was fabricated by first removing the bottom of a 5 mm quartz cuvet (Fisher Scientific) using a masonry saw equipped with a silicon carbide wet cutting blade (Wale Apparatus Company). Blocks of RVC (60 ppi, Electrosynthesis Company) were cut to dimensions of ca. 20x10x5 mm and inserted through opposite ends of the cuvet after first adding a roughly 10 mm thick plug of glass wool to serve as a separator between the two electrodes. Sealing gaskets for the cuvet were prepared by folding paraffin wax film (American Can Company) to dimensions of ca. 20x15x5 mm, inserting a bent segment of 0.25 mm dia. Pt wire prior to the final folding to provide electrical contact to the RVC. A solution inlet/outlet hole of roughly 2 mm dia. was punched into the center of each wax gasket with a small screwdriver, and the gaskets were press-fitted to the ends of the cuvet. Teflon tubing (3 mm o.d. x 1 mm i.d., Dionex) was flared and sealed to the gasket's inlet/outlet holes using a flexible steel C-clamp and two nut/bolt assemblies. After finger tightening the clamp, water was pumped through the cell as the clamp was further tightened until there was no evidence of leakage. Bubbles trapped within the pores of the RVC were removed by dissolution in thoroughly degassed water that was pumped through the cell for a few hours, and care was taken to avoid reintroduction of air during subsequent use of the cell.

Instrumentation. Electrochemical measurements were performed using either a BioAnalytical Systems CV-50W volatmmetric analyzer or a BAS CV-27 voltammograph. Spectroscopic measurements were made with a Sciencetech modular spectrophotometer configured for transmittance sampling with a water-cooled 75 W xenon lamp, 1200 lines/mm grating monochromator, and a

multialkaline PMT detector (Hamamatsu model R508). A Perkin-Elmer series 10 HPLC pump and a Rheodyne model 7010 loop injector (0.1 mL sample loop) were used for flow measurements.

Procedure. The cell was clamped to a ring stand and aligned in the spectrometer sample chamber such that the source beam passed through the working RVC electrode and cast a slit image perpendicular to the sample flow path as depicted in Figure 1. This perpendicular orientation was chosen to enhance sample band resolution, minimize optically sampled solute concentration gradients, and permit variation in the cell's optical observation point along the sample flow axis (see "Conclusions" section below). The sample outlet tubing and an AgCl/Ag reference electrode (BAS) were immersed in a small sidearm flask containing electrolyte solution and a waste drain tube. For batch measurements, the sample inlet tube was connected to a standard Luerlok adapter to permit syringe filling of the cell, and the source beam was positioned near the upstream edge of the electrode to minimize the sample volume required to avoid memory effects. This minimal sample volume was determined to be roughly 3 mL under the employed conditions, with 5 mL volumes typically used to insure thorough flushing of the previous sample. Potential difference absorbance measurements were made referenced to a single beam measurement of the analyte solution obtained at the cited electrode potential. For flow injection experiments, the sample inlet tube was connected to the outlet of the LC pump's loop injector, and the source beam was positioned near the electrode's downstream edge (see Figure 1) to maximize analyte residence time within the RVC, hence maximizing analyte conversion,[14] prior to spectral observation. Though not reported here, the cell may likewise be used with the source beam at other positions along the flow axis (see "Conclusions" section), including downstream spectral observations (this would require removal of the glass wool separator and alignment of the source beam between the working and auxiliary RVC electrodes). Absorbance measurements were made versus a reference obtained while electrolyte solution was pumped through the cell at the selected flow rate.

RESULTS AND DISCUSSION

Batch Measurements. Shown in the lower half of Figure 2 is a cyclic voltammogram for 0.9 mM ferricyanide measured in the SEC cell. The observed voltammetric peak separation of roughly 100 mV is typical for RVC electrodes and is likely a result of restricted solution current paths.[6] Averaging the cathodic and anodic peak potentials gives an estimate of the redox couple's formal potential of ca. +0.250 V (vs. AgCl/Ag). The upper half of Figure 2 shows the voltabsorptogram for a similar solution measured by monitoring absorbance at 420 nm (versus a single beam measurement of the solution at 600 mV) while scanning the working electrode potential from 600 mV to -200 mV. Using these data, the Nernst equation was plotted and found to be linear ($r > 0.99$), yielding values for n and $E^{o'}$ of 1.01 and 0.248 V, respectively, in good agreement with the voltammetric results and previously reported values.[16]

Figure 3 shows the results of a double potential step chronoabsorptometric measurement for the ferri/ferrocyanide couple. Absorbance at 420 nm was measured at 1 s intervals as the working electrode potential was stepped first from -200 to 600 mV, causing the oxidation of ferrocyanide, and then back to -200 mV, causing the reduction of ferricyanide. The plot of absorbance change versus time shown in the lower half of this Figure is indicative of thin layer electrochemical behavior, while the first derivative of this plot (upper half of Figure) more clearly indicates that exhaustive electrolysis is achieved in approximately four minutes, a time consistent with expectations for 60 ppi RVC.[6]

Flow Measurements. To demonstrate use of the cell for flow measurements, absorbance at 420 nm was monitored for triplicate 0.1 mL injections of 10 mM ferricyanide with the working electrode potential held at 600 mV (no electrolysis), followed by triplicate injections at -200 mV (mass transfer limited reduction of ferricyanide). The absorbance/time curves for such measurements at flow rates of 0.5, 1, 2, 3 and 4 mL/min are shown in the upper half of Figure 4. Comparison of the peak absorbances

obtained at 600 mV to absorbances measured in batch experiments indicates the cell generates large sample dispersion[17]

$$D = c_o / c_p \quad (1)$$

where c_o and c_p are the bulk and peak formal concentrations of ferricyanide, respectively, at all flow rates examined, ranging from roughly 60 to 80 under the employed conditions. Such large dispersion results from the cell's relatively large dead volume (estimated at roughly 0.5 mL)[6], and convective mixing[18] of the sample band as it flows through the porous electrode. This latter effect is likely exacerbated by the blunt coupling of the sample inlet tube to the RVC, resulting in relatively stagnant solution regions in the cuvet corners and subsequent turbulent dilution of samples entering the cell.

The degree of analyte conversion for the flow electrolysis described here may be defined as

$$R = [ferro]_p / c_p \quad (2)$$

where $[ferro]_p$ is the peak species concentration of the electrolysis product, ferrocyanide. The stoichiometry of the electrode reaction requires that

$$[ferro]_p + [ferri]_p = c_p \quad (3)$$

where $[ferri]_p$ is the species concentration of ferricyanide, hence the absorbance at 420 nm is given by

$$A = a_{ferro} b [ferro]_p + a_{ferri} b [ferri]_p \quad (4)$$

where b is the path length and a_{ferro} and a_{ferri} are absorptivities for ferrocyanide and ferricyanide, respectively, at 420 nm. Substitution of equations 3 and 2 into equation 4 yields

$$R = (A_{red} / A_{ox} - 1) / (a_{ferro}/a_{ferri} - 1) \quad (5)$$

where A_{ox} and A_{red} are absorbances measured with the working electrode potential at 600 mV and -200 mV, respectively. Since $a_{ferro} << a_{ferri}$ at 420 nm,[19] the above relation simplifies to

$$R = 1 - A_{red} / A_{ox} \quad (6)$$

Using the data from Figure 4, conversions were computed as percentages and plotted against flow rate, yielding the curve shown in the lower half of Figure 4. The expected increase in conversion with decreasing flow rate is observed, a result of longer analyte residence times within the porous cathode at slower flow rates.[14]

An interesting flow dynamic is exhibited by the cell as seen upon examination of the peaks measured at 600 mV, i.e., those unaffected by electrolysis. As the expected result of diffusional broadening, increased peak widths and decreased peak heights accompany a decrease in flow rate over the range of roughly 9 mL/min (additional data not shown) to 2 mL/min. Peak widths continue to increase as the flow rate is slowed further, but the trend in peak heights is reversed as illustrated by the signals measured at 2, 1 and 0.5 mL/min. This behavior may result from decreased convective mixing of the sample band (see above discussion) entering the porous RVC at lower flow rates, a behavior consistent with previous reports of a change in flow characteristics observed in similar cells at flow rates near 2 mL/min.[14, 15]

CONCLUSIONS

In summary, a cell suitable for both batch and flow injection SEC measurements has been described. Its simple construction, favorable performance traits, and versatility make it an attractive alternative to the few previously reported cells of similar function. Regarding versatility, note that the design reported here permits spectral observation in all three possible modes, i.e., batch, flow with observation through the OTE, and flow with downstream observation (in which case the RVC's optical characteristics aren't relevant). Some important features of the present and the two most comparable previously reported cells are summarized in the Table below.

Considering the relevant tabulated traits, a rough comparison of the cells' sensitivities and detection limits can be made. A typical definition for limit of detection, LOD, is

$$LOD \equiv 3s_b / m \qquad (7)$$

where s_b is the background signal standard deviation and m is the calibration sensitivity. Though the s_b term will depend somewhat upon the cell's RVC porosity, it is determined primarily by properties of the employed spectrometer. The SEC cell trait that most significantly affects detection limits is thus its sensitivity. For potential difference SEC measurements of the simple type described here and in the cited references, [9,11] the theoretical calibration sensitivity for batch assays may be estimated from Beer's law as

$$m_{batch} \equiv A/c_o = \Delta\varepsilon b \tag{8}$$

and the flow sensitivity may likewise be estimated as

$$m_{flow} \equiv A/c_p = \Delta\varepsilon bR / D \tag{9}$$

where $\Delta\varepsilon$ is the difference in molar absorptivities for the analyte and its electrolysis product at the analytical wavelength. Detection limits for batch SEC determination of a given analyte are thus determined primarily by cell path length, while detection limits in flow mode depend additionally upon the cell's dispersion and conversion. Using the above equations and the tabulated data, relative detection limits for the present and similar cells operating in flow mode were estimated as flow sensitivity ratios,

$$\text{relative LOD} = m_{flow}\text{ (present cell)} / m_{flow}\text{ (cited cell)} \tag{10}$$

and are given in the Table.

Regarding the inferior dispersion and detection limit parameters estimated for the present cell, it is important to note that these quantities were determined for spectral observation near the downstream edge of the OTE. This location was selected in order to maximize conversion efficiency, which increases with distance traveled by the solute through the electrode.[14] Unfortunately, dispersion also increases with solute travel distance, hence the optimal observation point will be that for which the R/D ratio is maximal, not necessarily that corresponding to maximal R. Since both conversion and

dispersion vary with flow rate, the optimal observation point will likewise be flow rate dependent. A further advantage to the present cell design in this context is thus the ability to vary continuously the source beam position along the flow axis from the upstream to downstream edges of the OTE, allowing one to optimize sensitivity for a given set of experimental conditions.

ACKNOWLEDGMENTS

The authors gratefully acknowledge financial support of this work by the National Science Foundation, Washington, DC (grant CHE0079041).

FIGURES AND FIGURE CAPTIONS

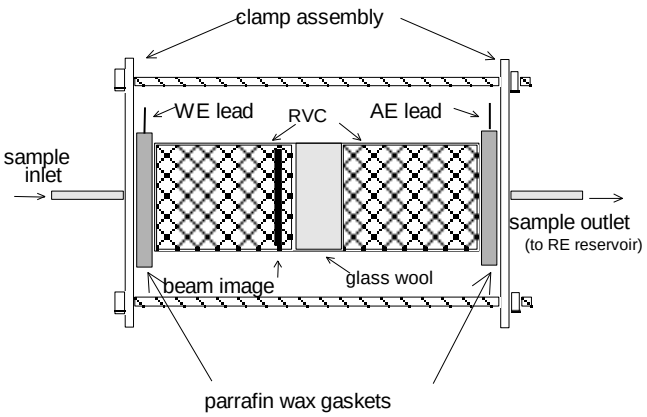

Figure 1. Diagram of the SEC cell.

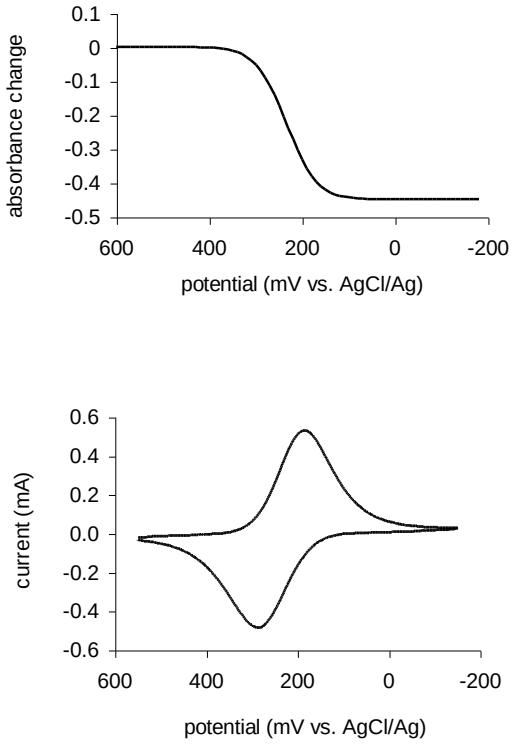

Figure 2. Voltabsorptogram (upper) and cyclic voltammogram (lower) for 0.9 mM potassium ferricyanide in 1 M potassium nitrate measured in the SEC cell at 1 mV/s scan rate.

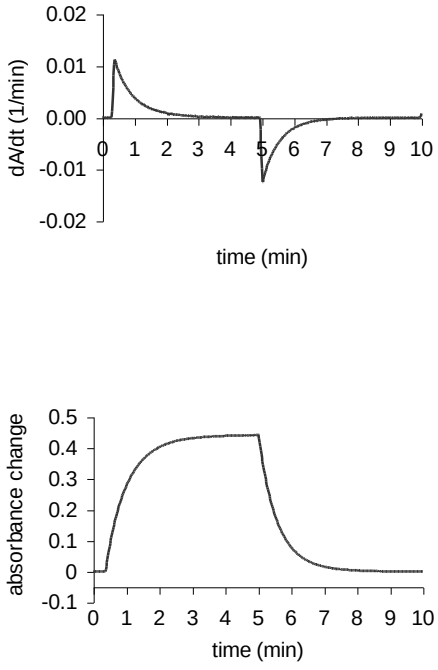

Figure 3. Plots of absorbance change versus time (lower) and its first derivative (upper) for double potential step experiments (-200 mV to 600 mV to -200 mV) of the same system as in Figure 2.

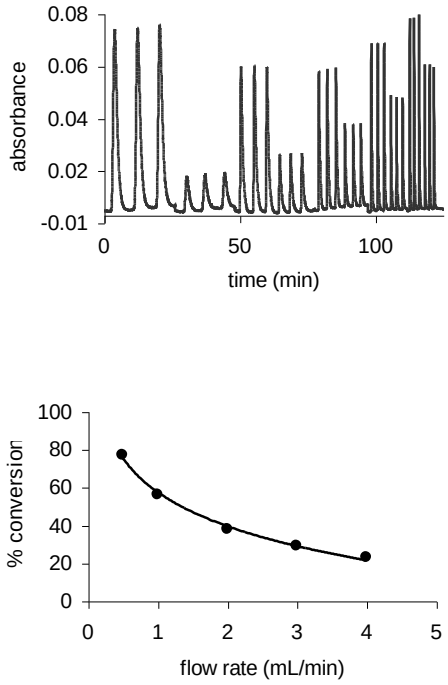

Figure 4. Absorbance-time curves (upper) for sequential triplicate injections of 10 mM potassium ferricyanide in 1 M potassium nitrate at alternating potentials of 600 mV and -200 mV and increasing flow rate (left-to-right). Plot of conversion versus flow rate (lower) derived from the A/t curves.

Table. Comparison of Traits for Similar SEC Cells

cell design	observation mode(s)*	RVC porosity (ppi)	path length (cm)	approximate dispersion	conversion at 0.5 mL/min (%)	relative flow LOD****
this work	b, d, e	60	0.5	70**	78**	1
ref 9	b, e	60	0.2	3***	38	0.2
ref 11	d	100	0.1	2***	22	0.5

* b=batch; d=flow, downstream observation; e=flow mode, observation through RVC
** for observation through the RVC near its downstream edge
*** estimated from data provided in the referenced publication
**** see text for details

Literature Cited

1. Kuwana, T.; Darlington, R. K.; Leedy, D. W. *Anal. Chem.* **1964**, 36, 2023.

2. Anderson, J.L.; Coury, L.A. Jr.; Leddy, J. *Anal. Chem.* **2000**, *72*, 4497-4520.

3. Gale , R. J., Ed. "Spectroelectrochemistry: Theory and Practice"; Plenum: New York, 1988.

4. Slaterbeck, A.F.; Stegemiller, M.L.; Seliskar, C.J.; Ridgway, T.H. and Heineman, W.R. *Anal. Chem*. **2000**, *72*, 5567-5575 (and references therein).

5. Norvell, V.E.; Mamantov, G. *Anal. Chem.* **1977**, *49*, 1470-1472.

6. Sorrels, J.W.; Dewald, H.D. *Anal. Chem.* **1990**, *62*, 1640-1643.

7. Armalis, S.; Kubiliene, E. *Anal. Chim. Acta* **2000**, *423*, 287-291.

8. Torimura, M.; Mochizuki, M.; Kano, K.; Ikeda, T.; Ueda, T. *Anal. Chem.* **1998**, *70*, 4690-4695.

9. Sorrels, J.W.; DeWald, H.D. *Electroanalysis* **1992**, *4*, 487-493.

10. Wieck, H.; Heider, G.; Yacynych, A.M. *Anal. Chim. Acta* **1984**, *158*, 137.

11. DeWald, H.D.; Wang, J. *Anal. Chim. Acta* **1984**, *166*, 163-170.

12. Wang, J.; DeWald, H. *Anal. Chem.* **1983**, *55*, 933.

13. Strohl, A.; Curran, D. *Anal. Chem.* **1979**, *51*, 1045.

14. Blaedel, W.; Wang, J. *Anal. Chem.* **1979**, *51*, 739.

15. Sioda, R.E. *Electrochim. Acta* **1970**, *15*, 783.

16. Kolthoff, I.M.; Tomsicek, W.J. *J. Phys. Chem.* **1935**, *39*, 945-954.

17. Skoog, D.A.; Holler, F.J.; Nieman, T.A. "Principles of Instrumental Analysis", fifth edition; Harcourt Brace College Publishers: Philadelphia, 1998; p. 836.

18. Willard, H.H.; Merritt, L.L., Jr.; Dean, J.A.; Settle, F.A., Jr. "Instrumental Methods of Analysis", sixth edition; Wadsworth Publishing Company: Belmont, CA, 1981; p. 442.

19. Winograd, N.; Blount, H.N.; Kuwana, T. *J. Phys. Chem.* **1969**, *73*, 3456-3462.